Synthesis and ^{13}C CPMAS NMR Characterization of Novel Thiophene-Based Nematogens

T. Narasimhaswamy,*,† N. Somanathan,‡ D. K. Lee,† and A. Ramamoorthy*,†

Department of Chemistry and Biophysics Research Division, University of Michigan, Ann Arbor, Michigan 48109-1055, and Polymer Laboratory, Central Leather Research Institute, Adayaru, Chennai, Tamil Nadu, India

Received September 5, 2004. Revised Manuscript Received December 8, 2004

The synthesis and characterization of novel thermotropic liquid crystals based on thiophene are reported. In these molecules, a thiophene ring, 1−4 disubstituted phenyl rings, and ester and azomethine linking units form the core fragment, and an alkoxy unit serves as the terminal group. All compounds exhibited an enantiotropic nematic phase, as confirmed by hot-stage polarizing microscope analysis and differential scanning calorimetry. Isotropic ^{13}C chemical shift values measured from CPMAS experiments on crystalline solid and nematic phases were compared to the values obtained from the static nematic phase. These experiments demonstrate the alignment of molecules in the magnetic field. Lower melting and clearing values are observed when two phenyl rings are part of the mesogen, while the addition of a third phenyl ring increases these values.

Introduction

The design of novel thermotropic liquid crystals as advanced functional materials involves suitable selection of a core fragment, linking group, and terminal functionality.[1] Among the known calamitic liquid crystals, a 1−4 disubstituted phenyl ring serves as a major core unit.[2] Incorporation of a 1−4 disubstituted phenyl ring-based core molecule ensures the structural linearity and overall high molecular polarizability that are major requirements for a molecule to exhibit mesomorphism.[2] However, with the discovery of banana liquid crystals, where bent molecules serve as a core, interest in the incorporation of nonlinear units has gained importance.[3−7] In addition, the incorporation of a nonlinear unit in the core should reduce the melting point of the resultant mesogen.[8] Among the nonlinear fragments, heterocyclic five-membered rings are notable.[2] Thiophene, a five-membered sulfur containing heterocycle, has recently attracted the attention of many research groups.[9−15] The incorporation of thiophene as a core fragment in the mesogen is known to contribute to an increase of optical anisotropy, a decrease of the melting point, a promotion of a negative dielectric anisotropy, a reduction in viscosity, and fast switching times.[7,15] Moreover, thiophene is a well-known structural fragment of conjugated polymers[16−18] which have gained importance for their potential applications in nonlinear optical materials,[19,20] organic light emitting diodes,[21,22] thin-film transistors,[23,24] molecular switches,[25,26] and filters.[27,28] The recent developments in functional liquid crystals demand materials that can emit polarized light for their applications as more efficient liquid crystal displays.[1,29,30] This particular

* To whom correspondence should be addressed. Tel.: (734) 647-6572. Fax: (734) 615-3790. E-mail: ramamoor@umich.edu (A.R.).
† University of Michigan.
‡ Central Leather Research Institute.

(1) O'Neill, M.; Kelly, S. M. *Adv. Mater.* **2003**, *15*, 1135.
(2) Neubert, M. E. In *Liquid Crystals-Experimental Study of Physical Properties and Phase Transitions*; Kumar, S., Ed.; Cambridge University Press: Cambridge, U.K., 2001; Chapter 10, p 393.
(3) Pelzl, G.; Diele, S.; Weissflog, W. *Adv. Mater.* **2003**, *11*, 707.
(4) Eichhorn, S. H.; Paraskos, A. J.; Kishikawa, K.; Swager, T. M. *J. Am. Chem. Soc.* **2002**, *124*, 12742.
(5) Levitsky, I. A.; Kishikawa, K.; Eichhorn, S. H.; Swager, T. M. *J. Am. Chem. Soc.* **2000**, *122*, 2474.
(6) Paraskos, A. J.; Swager, T. M. *Chem. Mater.* **2002**, *14*, 4543.
(7) Campbell, N. L.; Duffy, W. L.; Thomas, G. I.; Wild, J. H.; Kelly, S. M.; Bartle, K.; O'Neill, M.; Minter, V.; Tuffin, R. P. *J. Mater. Chem.* **2002**, *12*, 2706.
(8) Wu, L.-H.; Wang, Y.-C.; Hsu, C.-S. *Liq. Cryst.* **2000**, *27*, 1503.
(9) Matharu, A. S.; Grover, C.; Komitovb, L.; Andersson, G. *J. Mater. Chem.* **2002**, *10*, 1303.
(10) Zhang, H.; Shiino, S.; Shishido, A.; Kanazawa, A.; Tsutsumi, O.; Shiono, T.; Ikeda, T. *Adv. Mater.* **2000**, *12*, 1339.
(11) Kiryanov, A. A.; Seed, A. J.; Sampson, P. *Tetrahedron Lett.* **2001**, *57*, 5757.
(12) Yamada, T.; Azumi, R.; Tachibana, H.; Sakai, H.; Abe, M.; Bäuerle, P.; Matsumoto, M. *Chem. Lett.* **2001**, 1022.
(13) Pantalone, K.; Seed, A. J. *Liq. Cryst.* **2002**, *29*, 945.
(14) Carella, A.; Castaldo, A.; Centore, R.; Fort, A.; Sirigu, A.; Tuzi, A. *J. Chem. Soc., Perkin Trans. 2* **2002**, 1791.
(15) Sharma, S.; Lacey, D.; Wilson, P. *Liq. Cryst.* **2003**, *30*, 451.
(16) Guernion, N. J. L.; Hayes, W. *Curr. Org. Chem.* **2004**, *8*, 637.
(17) Granstrom, M. *Polym. Adv. Technol.* **1997**, *8*, 424.
(18) Roncali, J. *Chem. Rev.* **1992**, *92*, 711.
(19) Wei, Y.; Shaokui, C.; Zhanjia, H.; Luping, Y. *Macromolecules* **2003**, *36*, 7014.
(20) Massimiliano, L.; Luisa, P.; Costa-Bizzarri, P.; Della-Casa, C.; Alessandro, F. *Macromol. Rapid Commun.* **2002**, *23*, 630.
(21) Sheng-Han, W.; Chi-Hsien, S.; Jar-Hung, C.; Chia-Chen, H.; Raymond, T.; Chien-Chao, T. *J. Polym. Sci., Part A: Polym. Chem.* **2004**, *42*, 3954.
(22) Tingxi, L.; Takashi, Y.; Hsing-Lin, L.; Junji, K. *Polym. Adv. Technol.* **2004**, *15*, 266.
(23) Michael, L. H.; Jeng-Ping, L.; Robert, A. S.; Yiliang, W.; Ping, L.; Beng, S. O. *J. Appl. Phys.* **2004**, *96*, 2063.
(24) Joseph, K. R.; Michael, D. M.; Ekaterina, N. K.; Jinsong, L.; Frechet, J. M. J. *Adv. Mater.* **2003**, *15*, 1519.
(25) Bertarelli, C.; Gallazzi, M. C.; Lucotti, A.; Zerbi, G. *Synth. Met.* **2003**, *139*, 933.
(26) Lucas, L. N.; Jaap, J. D. D. J.; Jan, H. V. E.; Richard, M. K.; Ben, L. F. *Eur. J. Org. Chem.* **2003**, 155.
(27) Rong, H. L.; Chen, Y. H.; Chin-Ti, C. *J. Appl. Polym. Sci.* **2004**, *92*, 1432.
(28) Teruaki, H.; Shin, H. *Polym. Mater. Sci. Eng.* **2003**, *88*, 152.

10.1021/cm048494c CCC: $30.25
Published on Web 03/17/2005

application requires the incorporation of a mesogen in the molecule that has the capability to exhibit light emission. This could be achieved by suitable incorporation of a mesogenic unit in thiophene molecules, whose potential for use in organic light-emitting diodes is well known.[21,22]

In recent years, high-resolution solid-state ^{13}C NMR has acquired prime importance in the characterization of molecular, macromolecular, and supramolecular materials.[31,32] Many varieties of liquid crystals have been subjected to high-resolution solid-state NMR investigation as this technique provides information about structure, geometry, dynamics, and molecular packing in both crystalline solid and mesophase.[31−34] Because all of the advanced functional materials find their diverse applications in the solid state, detailed characterization of these materials by high-resolution solid-state NMR provides information of great importance in designing functional materials. This study focuses on the synthesis and characterization of novel thermotropic liquid crystals based on thiophene. Variable-temperature high-resolution solid-state ^{13}C NMR is employed for studying the structural changes in the solid state and the mesophase.

Experimental Section

Thiophene-3-carboxylic acid, thiophene-3-carboxaldehyde, 4-nitrophenol, stannous chloride, 4-hydroxy methyl benzoate, thionyl chloride, dicyclohexyl carbodiimide, 4-hydroxy benzaldehyde, and 4-dimethylamino pyridine were purchased from Aldrich. 2-Butanone, ethanol, heptane, carbon tetrachloride, methanol, 2-propanol, acetonitrile, dioxane, dimethyl formamide (DMF), tetrahydrofuran, carbon tetrachloride, and diethyl ether were solvent grade and used without further purification.

Synthesis of 4-Butoxy Benzoic Acid (BBA) [3]. 4-Butoxy benzoic acid was prepared by a two-step procedure. In a typical experiment, 4-hydroxy methyl benzoate (395 mmol) was placed in a 1-L three-necked round-bottom flask equipped with a stirrer and a thermometer, and DMF (300 mL) and potassium carbonate (500 mmol) were added. The resulting mixture was stirred while maintaining the temperature at 90 °C, and *n*-butyl bromide (500 mmol) was added through a dropping funnel over a period of 30 min. The stirring was continued for 2 h, and the mixture was allowed to cool and then poured into a 2-L beaker. The contents were diluted with water (500 mL), transferred to a separating funnel, and diethyl ether was added. The ether layer was extracted using 10% NaOH solution and distilled water, and the organic layer was dried with anhydrous sodium sulfate. Upon the evaporation of ether, a colorless liquid 4-butoxy methyl benzoate (75 g, 91%) resulted.

4-Butoxy methylbenzoate (330 mmol) was placed in a 1-L single-necked round-bottom flask equipped with a double-wall water condenser. Ethanol (150 mL) and potassium hydroxide (850 mmol) dissolved in distilled water (150 mL) were added to the flask. The solution was refluxed for 1 h and allowed to cool to room temperature. It was then neutralized with 1 N HCl to get a white precipitate. The solid was recrystallized from carbon tetrachloride. Yield: 93%. mp: 147 °C. IR (KBr, cm^{-1}): 3070, 2955, 2872, 2666, 2452, 1679, 1604, 1256, 1171. ^1H NMR (500 MHz, $CDCl_3$): δ 11.41, 8.05, 6.93, 4.02, 1.79, 1.54, 0.98. ^{13}C NMR (125 MHz, $CDCl_3$): δ 172.17, 163.78, 132.43, 121.48, 114.26, 68.05, 31.20, 19.27, 13.9.

4-Butoxy Benzoic Acid 4-Nitro-phenyl Ester (BBNP) [4]. In a representative experiment, BBA (50 mmol) and 4-nitrophenol (50 mmol) were placed in a conical flask (1 L). THF (150 mL) was added to the flask, and the contents were dissolved. Dicyclohexyl carbodiimide (50 mmol) in THF (50 mL) was added while stirring the solution. 4-Dimethylamino pyridine (5 mmol) was added subsequently, and stirring was continued at room temperature overnight. Filtration of solid dicyclohexyl urea and evaporation of the solvent resulted in a yellow solid that was purified by recrystallization from heptane. Yield: 66%. mp: 57 °C. IR (KBr, cm^{-1}): 3110, 3085, 2969, 2943, 2876, 1738, 1607, 1528, 1265, 1169. ^1H NMR (500 MHz, $CDCl_3$): δ 8.26, 8.11, 7.36, 6.97, 4.03, 1.79, 1.50, 0.98. ^{13}C NMR (125 MHz, $CDCl_3$): δ 164.15, 163.88, 156.06, 145.25, 132.58, 125.25, 122.75, 120.44, 114.59, 68.30, 31.18, 19.27, 13.92.

4-Butoxy Benzoic Acid 4-Amino-phenyl Ester (BBAP) [5]. BBNP (50 mmol), stannous chloride (250 mmol), and absolute ethanol (150 mL) were gently refluxed for 1 h. The resulting solution was allowed to cool to room temperature and was neutralized with 10% aqueous sodium hydroxide solution to pH 7. The fine precipitate formed was filtered and dried in a vacuum oven for 12 h. The dried solid was stirred with acetone (500 mL) for 2 h, and the insoluble solid was filtered. Evaporation of acetone yielded BBAP, which was purified by recrystallization from heptane. Yield: 76%. mp: 95 °C. IR (KBr, cm^{-1}): 3453, 3336, 2959, 2938, 2874, 1711, 1605, 1511, 1276, 1173. ^1H NMR (500 MHz, $CDCl_3$): δ 8.13, 6.96, 6.69, 4.03, 3.67, 1.81, 1.51, 0.99. ^{13}C NMR (125 MHz, $CDCl_3$): δ 165.67, 163.48, 144.34, 143.21, 132.27, 122.45, 121.91, 115.78, 114.33, 68.07, 31.23, 19.3, 13.95.

4-[Thien-3-ylmethylene]amino]phenyl-4-butoxybenzoate (TMAPB) [7]. A mixture of BBAP (10 mmol), thiophene-3-carboxaldehyde (10 mmol), and absolute ethanol (100 mL) was refluxed for 1 h. The resulting solid was filtered and washed with methanol (100 mL). The solid was dried in a vacuum oven and recrystallized from ethyl acetate. Yield: 70%. mp: 123.9 °C. IR (KBr, cm^{-1}): 3011, 2952, 2868, 1722, 1619, 1251, 1068. ^1H NMR (500 MHz, $CDCl_3$): δ 8.47, 8.13, 7.80, 7.70, 7.39, 7.23, 6.95, 4.05, 1.83, 1.53, 0.99. ^{13}C NMR (125 MHz, $CDCl_3$): δ 165.04, 163.54, 154.50, 149.56, 149.10, 140.73, 132.25, 130.31, 126.73, 125.90, 122.39, 121.48, 121.70, 114.28, 67.98, 31.11, 19.17, 13.79.

A similar strategy was used for synthesizing 4-[thien-3-ylmethylene]amino]phenyl-4-decyloxybenzoate homologue (TMADB).

4-Dodecyloxy benzoic acid 4-amino-phenyl ester (DdBAP) was synthesized using a procedure given above that was used to synthesize BBAP.

4-Dodecyloxy Benzoic Acid 4-[(4-Hydroxy-benzylidene)-amino]-phenyl Ester (DoBHBAP) [6]. A mixture of DdBAP (10 mmol), 4-hydroxy benzaldehyde (10 mmol), and absolute ethanol (100 mL) was refluxed for 1 h. The resulting solid was filtered, washed with methanol (100 mL), dried in a vacuum oven, and purified by recrystallization from 50:50 2-propanol:methanol. Yield: 63%. mp: 120 °C. IR (KBr, cm^{-1}): 3361, 2919, 2851, 1727, 1608, 1512, 1255, 1170. ^1H NMR (500 MHz, $CDCl_3$): δ 8.46, 8.03, 7.97, 7.23, 7.22, 6.83, 4.05, 1.72, 1.31, 0.83. ^{13}C NMR (125 MHz, $CDCl_3$): δ 165.23, 163.58, 161.26, 160.49, 150.13, 149.0, 146.84, 141.76, 132.43, 132.20, 131.12, 122.31, 122.14, 115.21, 114.81, 68.72, 68.66, 31.74, 29.45, 29.43, 29.38, 29.11, 22.55, 14.31.

4-([Thien-3-ylcarboxy)phenyl]methylene]amino)phenyl-4-dodecyloxybenzoate (TCPMAPDdB) [8]. In a representative experi-

(29) Kawamoto, M.; Mochizuki, H.; Ikeda, T. L. B.; Shirota, Y. *J. Appl. Phys.* **2003**, *94*, 6442.
(30) Grell, M.; Bradley, D. D. C. *Adv. Mater.* **1999**, *11*, 895.
(31) Spiess, H. W. *Macromol. Symp.* **2003**, *201*, 85.
(32) Brown, S. P.; Spiess, H. W. *Chem. Rev.* **2001**, *101*, 4125.
(33) Fung, B. M. *Prog. Nucl. Magn. Reson. Spectrosc.* **2002**, *41*, 171.
(34) Zimmermann, H.; Bader, V.; Poupko, R.; Wachtel, E. J.; Luz, Z. *J. Am. Chem. Soc.* **2002**, *124*, 15286.

Scheme 1. Multistep Synthetic Strategy of Thiophene Mesogens

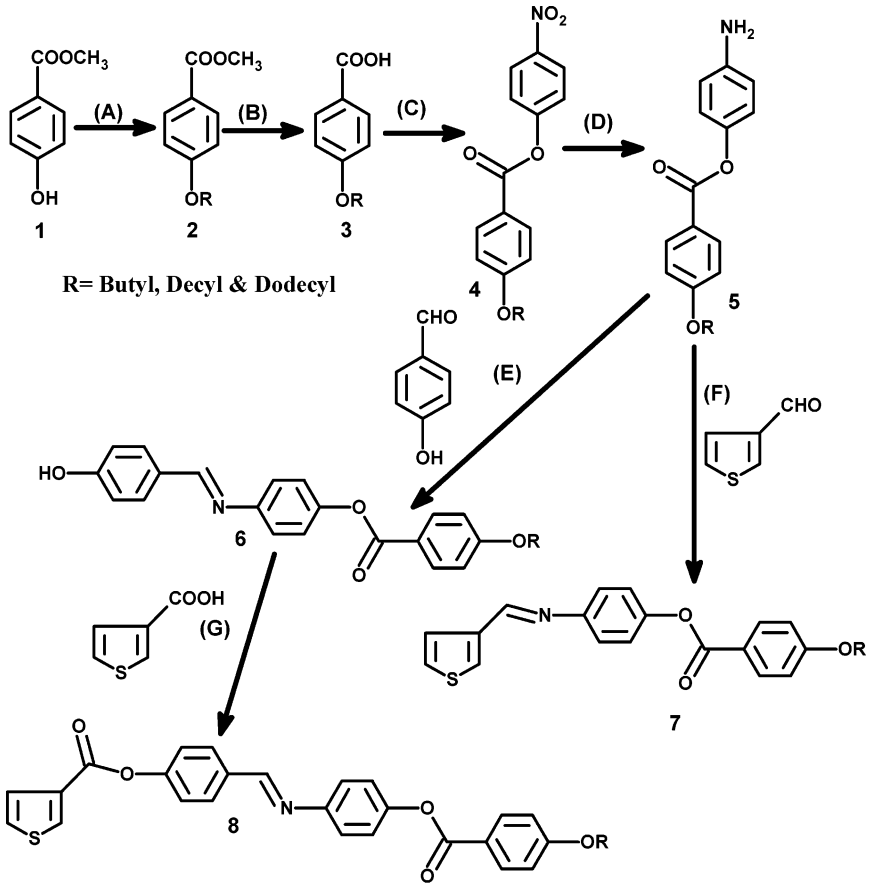

(A)=RBr/DMF/K_2CO_3; (B)=KOH/EtOH;
(C)=DCC/DMAP; (D)=$SnCl_2$/EtOH;
(E) & (F)=EtOH/Reflux; (G)=DCC/DMAP

ment, thiophene-3-carboxylic acid (50 mmol), DoBHBAP (50 mmol), and THF (150 mL) were placed in a 1 L conical flask. Dicyclohexyl carbodiimide (50 mmol) in THF (50 mL) and 4-dimethylamino pyridine (5 mmol) were added sequentially, and the stirring was continued at room temperature overnight. The insoluble dicyclohexyl urea was filtered, and the solvent was removed by evaporation. The solid thus obtained was recrystallized from ethyl acetate. Yield: 60%. mp 142 °C. IR (KBr, cm^{-1}): 3103, 2919, 2851, 1735, 1607, 1258, 1080. ^{1}H NMR (500 MHz, $CDCl_3$): δ 8.48, 8.33, 8.13, 7.96, 7.67, 7.34, 7.26, 6.98, 4.04, 1.81, 1.63, 1.31, 0.88. ^{13}C NMR (125 MHz, $CDCl_3$): δ 165.19, 163.65, 160.77, 159.33, 153.16, 149.45, 149.37, 134.48, 134.00, 132.4, 132.0, 130.18, 128.00, 126.3, 122.58, 122.31, 121.93, 121.5, 114.39, 68.42, 29.76, 29.75, 29.70, 29.67, 29.47, 26.0, 22.55, 14.26.

FT-IR spectra of all of the compounds were recorded in KBr-pellet form using a Nicolet Impact 400 spectrometer. ^{1}H and ^{13}C NMR spectra of the compounds in $CDCl_3$ or DMSO-d_6 solution were recorded on a JEOL 500 MHz instrument at room temperature using tetramethylsilane as an internal standard. The resonance frequencies of ^{1}H and ^{13}C were 500.15 and 125.76 MHz, respectively. All solid-state ^{13}C CPMAS NMR experiments were performed on a Chemagnetics/Varian Infinity 400 MHz solid-state NMR spectrometer equipped with a 9.4 T wide-bore JMT magnet. Resonance frequencies of ^{13}C and ^{1}H nuclei were 100.65 and 400.14 MHz, respectively. A 5 mm Chemagnetics double resonance probe and a 5 mm zirconia rotor were used. All samples were recrystallized from ethyl acetate and vacuum-dried before use. ^{13}C spectra were obtained at either 6 or 9 $\pm$ 0.001 kHz spinning speed using a ramp-CP[35,36] pulse sequence with a 2 ms contact time, 75 kHz two-pulse phase modulation (TPPM) proton decoupling,[37] and a 3 s recycle delay. ^{13}C chemical shift frequencies are referenced to TMS by setting the observed ^{13}C signals of solid adamantane to 29.5 and 38.56 ppm. Experimental data were processed in a Sun Sparc computer using the Spinsight software (Chemagnetics). For FID workup, 2K data points were zero-filled to 16K points after apodization using a 50 Hz exponential line broadening. The temperature of the sample was maintained with an accuracy of 0.1 °C using a Chemagnetics temperature controller.

The nature of the mesophase and the temperature of occurrence were determined with an Olympus BX50 polarizing optical microscope equipped with a Linkam THMS 600 stage with a TMS 94 temperature controller. The photographs were taken using an Olympus SLR camera. Differential scanning calorimetry (DSC) traces were recorded in nitrogen atmosphere using a Perkin-Elmer DSC 7 instrument with a heating rate of 10 °C/min. Each sample was subjected to two heating and two cooling cycles.

Results and Discussion

Novel thermotropic liquid crystals consisting of thiophene and 1−4 disubstituted phenyl rings as core fragments, ester and azomethine as linking units, and an alkoxy group as a

(35) Metz, G.; Wu, X.; Smith, S. O. *J. Magn. Reson., Ser. A* **1994**, *110*, 219.
(36) Shekar, S. C.; Lee, D. K.; Ramamoorthy, A. *J. Magn. Reson.* **2002**, *157*, 223.
(37) Bennett, A. E.; Rienstra, C. M.; Auger, M.; Lakshmi, K. V.; Griffin, R. G. *J. Chem. Phys.* **1995**, *103*, 6951.

Scheme 2. Chemical Structures of TMADB and TCPMAPDdB

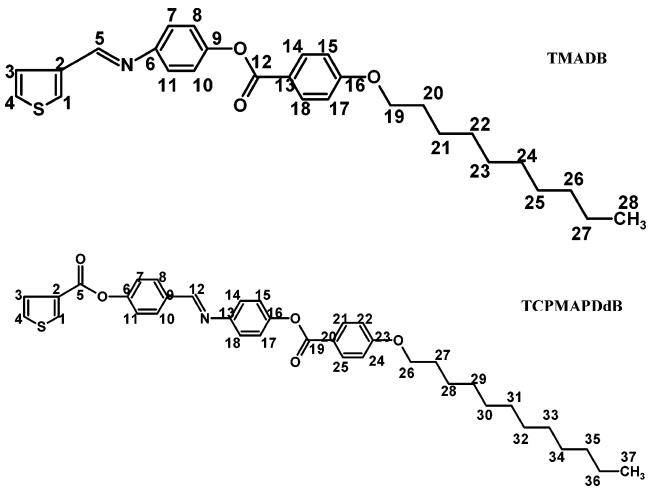

terminal functionality have been synthesized, as depicted in Scheme 1. The intermediates such as alkoxy benzoic acids[38] and alkoxy benzoic acid-4-nitrophenyl esters[39] are known for their mesogenic behavior. This nitro compound upon reduction using a reported procedure[40] resulted in an amine compound that showed no liquid crystalline property. On the other hand, one of the intermediates DoBHBAP [**6**], which has not been reported in the literature, exhibited an enantiotropic nematic phase. The crystal to nematic phase transition temperature (T_{C-N}) of this new compound is 120 °C, and its nematic to isotropic phase transition temperature (T_{N-I}) is 147 °C. In contrast to other functional groups, the hydroxyl is not a good terminal group and, in view of that, observation of an enantiotropic nematic phase in DoBHBAP is significant, as it would serve as a donor for hydrogen-bonding liquid crystals.

Thiophene-based liquid crystals are gaining importance in view of their potential applications as functional liquid crystals.[9−15] From the structural point of view, the mesogen in thiophene compounds can be introduced in the 2, 5, or 3 position. Thermotropic liquid crystals of thiophene substituted at either 2 and 5 or 3 positions have been reported in the literature.[4−8] The 2,5 substitution results in bent core mesogens and have received considerable attention by many researchers.[4−8] However, 3-substitution facilitates the development of dimeric, oligomeric, and polymeric thiophenes as 2,5-centers are available for further modification. The present study focuses on the synthesis of two classes of 3-substitued thiophene liquid crystals (TMAPB, TMADB, and TCPMAPDdB (Scheme 2)).

TMAPB ($C_{22}H_{21}NO_3S$) and its homologue TMADB ($C_{28}H_{33}NO_3S$) are structurally similar except that the terminal alkoxy chain of TMAPB is 6-carbons shorter than TMADB (Scheme 2). These two compounds are different from TCPMAPDdB ($C_{37}H_{41}NO_5S$), as the latter consists of an additional 1−4 disubstituted phenyl ring and an ester group (Scheme 2). All three compounds exhibited an enantiotropic

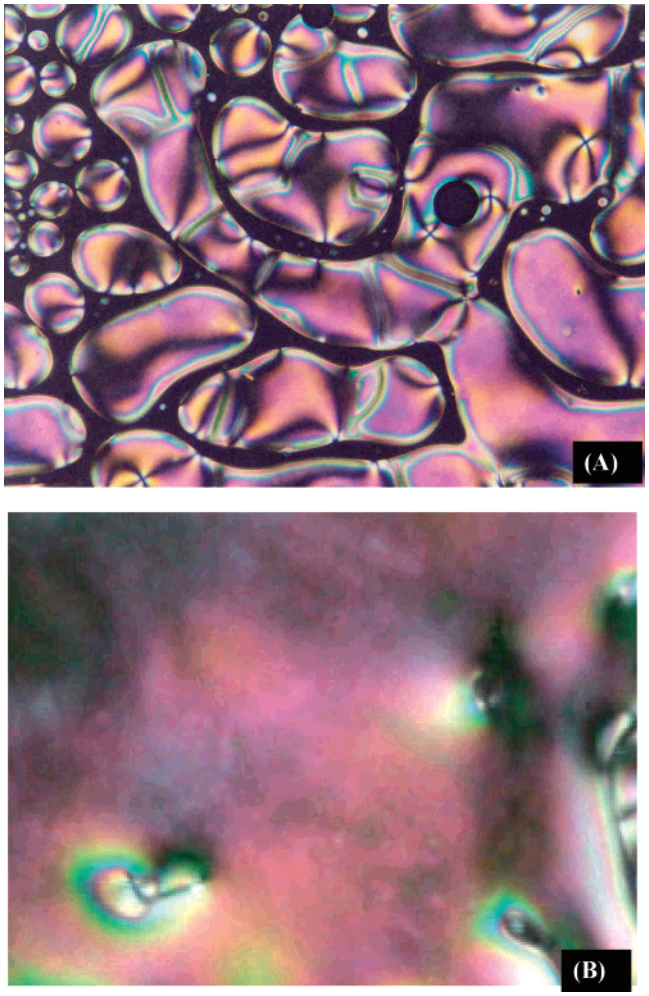

Figure 1. Polarizing microscope photographs: (A) nematic phase of TMADB at 135.2 °C while cooling; (B) nematic phase of TCPMAPDdB at 255 °C while cooling.

nematic phase as observed from the hot-stage polarizing microscope study (Figure 1). Figure 1 shows the characteristic nematic phase texture of TMAPB and TCPMAPDdB. The appearance of nematic phase in TMAPB and TCPMAPDdB is attributed to their common terminal units. Phase transition temperatures, change in the transition enthalpy, and the phase stability values for these compounds determined from DSC experiments are given in Table 1. The change in the transition enthalpy (ΔH) at T_{C-N} and T_{N-I} further supports the occurrence of a nematic phase in all of these compounds. The values of T_{C-N} and T_{N-I} are in the following order: TCPMAPDdB > TMAPB > TMADB. It is clear that the addition of a phenyl ring and an ester group increases the phase temperature and phase stability values (Table 1). The higher phase stability value for TCPMAPDdB indicates the high molecular polarizability of the compound. The relatively lower melting point and phase stability values measured for TMAPB and its homologue TMADB are consistent with the trend observed for other thiophene-based liquid crystals.[7,15]

The ^{13}C CPMAS (cross polarization magic angle spinning) NMR spectra of TMAPB, TMADB, and TCPMAPDdB are shown in Figures 2, 3, and 4, respectively. The chemical shift values measured from Figures 2 and 3 are given in Table 2. The carbon numbering of the molecular structure is shown in Scheme 2. Based on the substitution pattern of the core

(38) Gray, G. W.; Jones, B. *J. Chem. Soc.* **1954**, 683.
(39) Griffin, A. C.; Fisher, R. F.; Havens, S. J. *J. Am. Chem. Soc.* **1978**, *100*, 6329.
(40) Bellamy, F. D.; Ou, K. *Tetrahedron Lett.* **1984**, *25*, 839.

Table 1. DSC Data of Thiophene-Based Nematogens

compound	T_{C-N} (°C)	T_{N-I} (°C)	change in enthalpy ΔH (kcal/mol) T_{C-N} (°C)	change in enthalpy ΔH (kcal/mol) T_{N-I} (°C)	phase stability (°C)
TMAPB	124 ± 0.2	153.8 ± 1.8	7.43 ± 0.2	0.26 ± 0.2	29.8 ± 1.7
TMADB	91.5 ± 0.2	137.2 ± 0.5	8.01 ± 0.6	0.26 ± 0.2	45.7 ± 0.7
TCPMAPDdB	141.7 ± 0.5	263.2 ± 0.7	6.62 ± 0.5	0.23 ± 0.1	121.5 ± 0.3

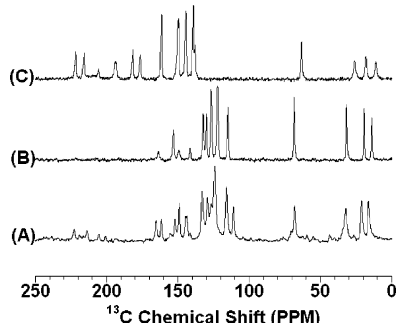

Figure 2. Carbon-13 NMR spectra of TMAPB: (A) 9 kHz MAS at 23 °C; (B) 6 kHz MAS at 130 °C; (C) under static condition at 130 °C. Spectra A, B, and C were obtained using 1352, 628, and 612 scans, respectively.

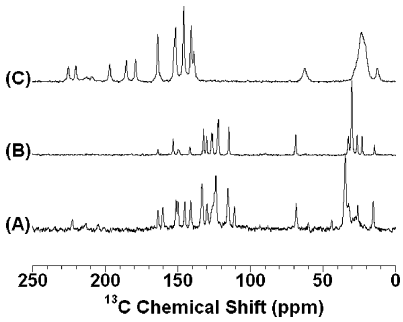

Figure 3. Carbon-13 NMR spectra of TMADB: (A) 9 kHz MAS at 23 °C; (B) 6 kHz MAS at 100 °C; (C) under static condition at 100 °C. Spectra A, B, and C were obtained using 1008, 260, and 580 scans, respectively.

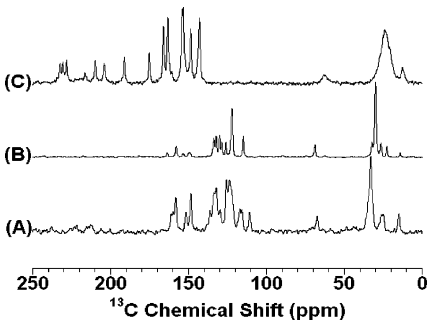

Figure 4. Carbon-13 NMR spectra of (TCPMAPDdB): (A) 9 kHz MAS at 23 °C; (B) 6 kHz MAS at 150 °C; (C) under static condition at 150 °C. Spectra A, B, and C were obtained using 2404, 604, and 1120 scans, respectively.

fragment in TMAPB and TMADB, 14 chemical shift peaks accounting for 18 carbons can be expected. The solution ^{13}C NMR spectra of both of these compounds show 14 peaks in the 110−170 ppm range for the thiophene and phenyl ring carbons as well as linking units (chemical shift values of TMAPB are given in the Experimental Section). In the CPMAS spectrum of TMAPB in the solid state (Figure 2A), chemical shift values of 11 peaks from the 18 carbons of the core fragment in the region 110−170 ppm match well with the solution NMR values. Fewer peaks observed in the solid state than in the liquid state is due to the poorly resolved resonances of phenyl ring carbons. This is clearly seen in

Table 2. ^{13}C CPMAS Chemical Shift Values (ppm) of TMAPB and TMADB

carbon number	TMAPB crystalline 23 °C	TMAPB nematic 130 °C	TMADB crystalline 23 °C	TMADB nematic 100 °C
1	129.4 ± 0.7	130.0 ± 0.3	132.7 ± 0.5	130.4 ± 0.2
2	143.7 ± 0.4	141.4 ± 0.5	141.0 ± 0.5	141.9 ± 0.2
3	126.4 ± 0.3	126.3 ± 0.2	126.2 ± 0.2	126.4 ± 0.2
4	126.9 ± 0.3	126.7 ± 0.2	126.2 ± 0.2	127.2 ± 0.3
5	152.2 ± 0.5	153.3 ± 0.5	154.4 ± 0.5	153.5 ± 0.2
6	149.1 ± 0.4	149.3 ± 0.9	148.9 ± 0.2	149.2 ± 0.2
7	124.1 ± 0.9	122.4 ± 0.3	124.3 ± 0.4	122.9 ± 0.3
8	124.1 ± 0.9	122.0 ± 0.3	123.3 ± 0.3	122.3 ± 0.3
9	149.1 ± 0.4	149.3 ± 0.9	150.2 ± 0.6	150.1 ± 0.2
10	124.1 ± 0.9	122.0 ± 0.3	123.3 ± 0.3	122.3 ± 0.3
11	124.1 ± 0.9	122.4 ± 0.3	124.3 ± 0.4	122.9 ± 0.3
12	165.4 ± 0.4	163.7 ± 0.6	165.7 ± 0.5	164.0 ± 0.2
13	124.1 ± 0.5	122.4 ± 0.3	123.3 ± 0.3	122.3 ± 0.3
14	133.2 ± 0.7	132.0 ± 0.4	133.3 ± 0.9	132.7 ± 0.2
15	115.9 ± 0.7	114.9 ± 0.4	116.2 ± 0.6	115.1 ± 0.2
16	161.7 ± 0.4	163.7 ± 0.6	164.9 ± 0.4	162.1 ± 0.1
17	115.9 ± 0.7	114.9 ± 0.4	116.2 ± 0.6	115.1 ± 0.2
18	133.2 ± 0.7	132.0 ± 0.3	133.3 ± 0.9	132.7 ± 0.2
19	68.2 ± 0.5	68.5 ± 0.3	68.1 ± 0.7	69.1 ± 0.3
20	32.3 ± 0.9	31.7 ± 0.3	35.0 ± 0.3	32.8 ± 0.3
21	21.4 ± 0.6	19.4 ± 0.2	33.4 ± 1.0	30.5 ± 0.4
22	16.6 ± 0.6	14.0 ± 0.3	33.4 ± 1.0	30.5 ± 0.4
23			33.4 ± 1.0	30.5 ± 0.4
24			33.4 ± 1.0	30.5 ± 0.4
25			33.4 ± 1.0	30.5 ± 0.4
26			26.7 ± 0.6	26.8 ± 0.3
27			25.3 ± 0.6	23.3 ± 0.2
28			15.4 ± 0.6	14.7 ± 0.2

Figure 2A, where the intense peak at 124.1 ppm accounts for several carbons. However, additional peaks observed in the aromatic region of the spectrum are attributed to different phenyl ring orientations present in the crystalline state at room temperature (Figures 2A, 3A, and 4A), which vanish in the liquid state as well as in the nematic phase (Figures 2B, 3B, and 4B). In the region 10−70 ppm, four peaks are noticed for TMAPB that are due to OCH_2, CH_2, and CH_3 of the terminal groups. In the case of TMADB (Figure 3A), the region 110−170 ppm is similar to that of TMAPB (Figure 2A), and there are seven peaks in the 10−70 ppm region.

The CPMAS NMR of TMAPB in the nematic phase (Figure 2B) also shows 11 peaks in the region 110−170 ppm and four peaks in the region 10−70 ppm. The chemical shift values are comparable to the solid-state spectrum (Table 2). However, in the case of TMADB (Figure 3B), 13 peaks are observed in the region 110−170 ppm and six peaks are observed for terminal alkoxy chain carbons.

The static spectra of both of the compounds (TMAPB and TMADB) in the nematic phase (Figure 2C and Figure 3C) showed characteristic alignment of the molecule in the magnetic field. The signals are sharp, particularly in the aromatic region (130−170 ppm), and more intense than the CPMAS spectra of both the solid (Figures 2A and 3A) and the nematic phase (Figures 2B and 3B). In addition, the chemical shift values are different from their values in the

Table 3. ^{13}C CPMAS Chemical Shift (ppm) Values of TCPMAPDdB

carbon number	crystalline 23 °C	nematic 150 °C
1	134.2 ± 0.6	134.1 ± 0.4
2	132.5 ± 0.7	132.6 ± 0.3
3	126.1 ± 0.7	128.9 ± 0.2
4	126.1 ± 0.7	126.4 ± 0.3
5	160.3 ± 0.7	164.0 ± 0.4
6	152.0 ± 0.6	153.8 ± 0.6
7	123.9 ± 0.9	122.4 ± 0.4
8	132.5 ± 0.7	132.6 ± 0.3
9	134.2 ± 0.6	134.0 ± 0.4
10	132.5 ± 0.7	132.6 ± 0.3
11	123.9 ± 0.9	122.4 ± 0.4
12	158.5 ± 0.6	158.3 ± 0.3
13	148.8 ± 0.5	149.1 ± 0.2
14	122.7 ± 0.8	122.4 ± 0.4
15	122.7 ± 0.8	122.4 ± 0.4
16	148.8 ± 0.5	149.7 ± 0.2
17	122.7 ± 0.8	122.4 ± 0.4
18	122.7 ± 0.8	122.4 ± 0.4
19	161.3 ± 0.5	164.0 ± 0.4
20	122.7 ± 0.8	122.4 ± 0.4
21	130.1 ± 0.7	130.4 ± 0.3
22	116.1 ± 0.6	115.2 ± 0.2
23	161.3 ± 0.5	164.0 ± 0.4
24	116.1 ± 0.6	115.2 ± 0.2
25	130.1 ± 0.7	130.4 ± 0.3
26	67.7 ± 0.6	69.2 ± 0.3
27	33.4 ± 0.8	32.6 ± 0.3
28	26.7 ± 0.5	26.8 ± 0.3
29	33.4 ± 0.8	30.4 ± 0.4
30	33.4 ± 0.8	30.4 ± 0.4
31	33.4 ± 0.8	30.4 ± 0.4
32	33.4 ± 0.8	30.4 ± 0.4
33	33.4 ± 0.8	30.4 ± 0.4
34	33.4 ± 0.8	30.4 ± 0.4
35	33.4 ± 0.8	30.4 ± 0.4
36	25.3 ± 0.7	23.1 ± 0.3
37	15.3 ± 0.6	14.4 ± 0.2

CPMAS spectra (Table 2). This is attributed to the homogeneous alignment of the molecules in the presence of an external magnetic field. Both TMAPB and TMADB show six peaks in the region 130−170 ppm. These peaks are from CH carbons of phenyl and thiophene rings. The precise assignment of peaks in the aligned spectra (Figures 2C and 3C) is difficult in the absence of chemical shift anisotropy tensor values. The tentative assignment is based on the relative peak intensities. The appearance of one peak each for ortho and meta carbons of phenyl ring indicates the rapid motion of phenyl ring with respect to the para axis. The large span of the chemical shift anisotropy tensors of thiophene, phenyl ring, carbonyl, and the N═CH carbons provides the high resolution of the peaks in this region of the spectrum. Relatively broad lines observed in the region 10−70 ppm are mainly due to the overlap of the signals from all of the methylene carbons that have similar (but not identical) orientation with respect to the magnetic field.

Figure 4A and B shows the ^{13}C CPMAS NMR spectra of TCPMAPDdB in the solid and nematic phases, respectively. The chemical shift values measured from the CPMAS experiments on solid-state and nematic phase TCPMAPDdB are given in Table 3. Due to the presence of the additional phenyl ring and ester carbonyl, more peaks are expected in the region 110−170 ppm in contrast to TMAPB (Figure 2) and TMADB (Figure 3). However, 12 peaks accounting for 25 carbons are noticed in the region 110−170 ppm of the solid-state spectrum (Figure 4A), while the solution spectrum shows 19 peaks (chemical shift values are given in the Experimental Section). As mentioned earlier, fewer peaks observed in the solid-state spectrum is primarily due to the residual broadening of the peaks. For instance, three broad peaks are seen in the 120−128 ppm range of the solid-state spectrum (Figure 4A), whereas six lines are noticed in the same region of the liquid-state spectrum (not shown). The terminal dodecyloxy carbons appeared in the region 10−70 ppm. The nematic phase CPMAS spectrum (Figure 4B) also shows 12 peaks in the region 110−170 ppm for the core fragment and linking groups and six peaks for the terminal unit in the region 10−70 ppm. The static nematic phase spectrum of TCPMAPDdB is shown in Figure 4C, and the spectral features are similar to those of TMAPB (Figure 2C) and TMADB (Figure 3C). Determination of order parameters for these nematogens at various temperatures using recently developed PISEMA (polarization inversion spin exchange at the magic angle)[41−44] and PITANSEMA (polarization inversion time averaged nutation spin exchange at the magic angle)[45] experiments is in progress.

Conclusion

The multistep synthesis of novel thiophene mesogens has been reported, and the appearance of an enantiotropic nematic phase was confirmed by microscopic and thermal methods. Lower melting and clearing temperatures were observed for mesogens containing two phenyl ring structures, while the addition of a third phenyl ring not only enhanced the melting and clearing temperatures, but also the phase stability. The appearance of the nematic phase was further supported by variable-temperature solid-state ^{13}C NMR experiments, where magnetic-field-induced alignment of the molecules was clearly observed.

Acknowledgment. This research was partially supported by funds from the National Science Foundation (CAREER Development Award to A.R). T.N. is on a sabbatical leave from the Central Leather Research Institute, India.

CM048494C

(41) Wu, C. H.; Ramamoorthy, A.; Opella, S. J. *J. Magn. Reson.* **1994**, *A109*, 270.
(42) Ramamoorthy, A.; Opella, S. J. *Solid State NMR Spectrosc.* **1995**, *4*, 387.
(43) Ramamoorthy, A.; Wu, C. H.; Opella, S. J. *J. Magn. Reson.* **1999**, *140*, 131.
(44) Ramamoorthy, A.; Wei, Y.; Lee, D. K. *Ann. Rep. NMR Spectrosc.* **2004**, *52*, 2.
(45) Lee, D. K.; Narasimhaswamy, T.; Ramamoorthy, A. *Chem. Phys. Lett.* **2004**, *399*, 359.